Journal of Renewable Energies

Revue des Energies Renouvelables

journal home page : https://revue.cder.dz/index.php/rer

Research Paper

Integration of PV Distributed Generator in Electrical Distribution System with Electric Vehicles Charging Stations Considering Uncertainties using Chaotic SSA Algorithm

Mohamed Zellagui [a,b,*], Adel Lasmari [c], Samir Settoul [c], Rachid Chenni [c]

[a] *Department of Electrical Engineering, École de Technologie Supérieure (ÉTS), University of Québec, Canada*

[b] *Department of Electrical Engineering, Faculty of Technology, University of Batna 2, Batna, Algeria*

[c] *Department of Electrotechnic, Mentouri University of Constantine 1, Constantine, Algeria*

A R T I C L E I N F O

Article history:
Received 07 December 2020
Accepted 03 April 2021

Keywords:
Photovoltaic DG source
EV charging stations
Daily load uncertainties
Electrical distribution system
Chaotic salp swarm algorithm
Multi-objective function

A B S T R A C T

The penetration of renewable energy resource units in the Electrical Distribution System (EDS) has gradually increased. In addition to that, the interest in the electrification of the transport sector has brought about increasingly significant incentives for the integration of Electric Vehicles Charging Station (EVCS). In this regard, the planning of the installation of PV source-based Distributed Generation (DG) units in EDS considering EVCS should be carefully considered to avoid stressing the EDS. This paper applied various Chaotic Salp Swarm Algorithm (CSSA) based various chaotic maps methods with the multi-objective functions that are considered minimizing simultaneous the Active Power Loss (APL), the Annual Losses Cost (ALC), and the Total Voltage Deviation (TVV) in EDS. The proposed algorithms are tested on a standard IEEE 69-bus system that is used to demonstrate the feasibility of the CSSA algorithm in allocating the DG units by considering the uncertainty of the power delivered by the DG as well as the variation of load demand and EVCS in 24 hours. Furthermore, the overall EDS performances are also enhanced with simultaneous placement of both devices.

* *Corresponding author, E-mail address: m.zellagui@ieee.org / m.zellagui@univ-batna2.dz*
Tel.: + 1 514 466 0226

ISSN: 1112-2242 / EISSN: 2716-8247

1. Introduction

The traditional transportation system, which includes an internal combustion engine, is the primary source of emissions. In recent years, there has been a rise in total consumer penetration of Electric Vehicles (EVs) to reduce air emissions and oil dependency in transportation [1].
The PV and EV are exciting developments for enhancing energy efficiency and increasing the share of renewable energy sources in EDS. Temporal modeling of PV power generation and EV Charging Stations (EVCSs) is relevant for many reasons, including urban planning and EDS design and service, when it comes to the implementation, usage, and device integration of these technologies [2]. The EV charging stations, when connected to the EDS, offer a wide range of applications. When attached to the EDS, the EVCSs can be used for a variety of purposes. The most critical topic in this regard is the Grid to Vehicle (G2V) service mode in the power generation and distribution sector for reducing electricity loss and emissions by concentrating on the incorporation of large-scale renewable resources [3].

1.1 Literature review

Many charging stations for EVs connected to the electric grid, will have a major impact on the EDS. Various researchers on the planning problems concerning DGs and EVCSs in EDS can be found in numerous literatures. In the literature, numerous techniques, and algorithms to this problem: applied Mixed Integer Non-Linear Programming (MINLP) to maximize the benefit of the PEV-parking lot's owner [4], Mixed integer second-order cone programming (MISOCP) for minimize various annual cost in EDS [5], MISOCP for minimizing the total losses with maximizing the total DG and EV charging station [6], Probabilistic method and fuzzy theory for minimisation of DG installation, and maintenance costs [7], Genetic algorithm (GA) for maximize the profit measured by its net present value [8], Particle Swarm Optimisation (PSO) for maximisation of annual revenue for the power supply company [9], Differential evolutionary particle swarm (DEEPSO) algorithm to minimised electricity markets and wind DG cost [10], Grasshopper Optimizer Algorithm (GOA) for energy loss and voltage stability indexes reduction [11], Artificial Bee Colony (ABC) algorithm to minimize the power loss [12], Salp Swarm Algorithm (SSA) to minimize the fluctuation in the DC-bus voltage to the grid [13], Improved Differential Evolutional Algorithm (IDEA) for reduction the investment cost [14], Hybrid Optimization platform HOMER to minimizing the total net present cost [15], and recently proposed Hybrid optimization algorithm for minimising the voltage deviation, with power loss and DGs costs [16].

1.2 Application SSA on RES problems

Recently, meta-heuristic algorithms have become surprisingly very popular and superior in solving various engineering problems. Salp swarm algorithm (SSA) is a new meta-heuristic algorithm introduced in 2017 [17].

Several researchers have applied the SSA algorithm for several practical applications in renewable energy topics: optimal control scheme for LVRT capability improvement of power grid-connected PV power plants [18], optimal fractional-order PID controller of a two-area power system integrated with small hydro plants [19], optimal PID parameters for load frequency control of hybrid RES with uncertainty [20], optimization of voltage source inverter controller in EDS with PV source [21], the energy management with emission of RES micro-grids to minimize the total operating cost [22], identifying the parameters of the electrical equivalent circuit of PV [23], optimal reconfiguration and RES planning in EDS for reducing the active power losses [24]. Also, optimal allocation of PV source and shunt capacitor in EDS for minimized the active power loss [25], optimal benefits of high PV penetration EDS with battery and capacity allocation [26], optimal MPPT control for variable speed WT generator based PMGA [27], and optimal MPPT control PV system under partial shading condition [28].

1.3 Contribution and organization

This paper addresses the optimal integration of multiple solar photovoltaic sourced DG units in EDS with insertion EV charging station various CSSA algorithms. The optimal integration is designed to minimize the following technical and economic parameters: Active Power Loss (APL), Annual Losses Cost (ALC), and Total Voltage Deviation (TVV). In this study, the optimal integration of renewable-based DGs was applied and tested on a standard IEEE 69-bus system considering the uncertainties of load demand, EVCS, and DGs throughout the day. The main reason for studying these proposed scenarios is to show the impact of the integration of multiple DGs into EDS considering the various uncertainties to make the study more realistic.

This paper contains five sections along with the references list, it is organized as follows: Section 2 provides the formulation of the problem and the formulation of the mathematical problem. The various Chaotic SSA applied are presented in section 3. The simulation results and discussion are presented in section 4. Finally, the conclusions and future extensions are discussed in section 5.

2. Problem Formulation

2.1 Multi-objective function

To optimally DG integration into the EDS, several objective functions are used. In this paper, the following three main OFs are considered:

The Active Power Loss (APL) on the distribution line connecting from bus *i* to bus *j* represented by [29-31]:

$$P_{Loss}(i,j) = \alpha_{ij}(P_iP_j + Q_iQ_j) + \beta_{ij}(Q_iP_j + P_iQ_j) \tag{1}$$

Where,

$$\alpha_{ij} = \frac{R_{ij}}{V_iV_j}\cos\left(\delta_i - \delta_j\right) \text{ and } \beta_{ij} = \frac{R_{ij}}{V_iV_j}\sin\left(\delta_i - \delta_j\right) \tag{2}$$

And,

$$APL = \sum_{i=1}^{N_{bus}} \sum_{j=2}^{N_{bus}} P_{Loss}(i,j) \tag{3}$$

$$OF_1 = min\left(\sum_{t=1}^{24} APL(t)\right) \tag{4}$$

Then, the Annual Losses Cost (ALC), which depends on the active power loss, can be calculated as follows [29]:

$$ACL(i,j) = P_{Loss}(i,j) \times K_P \times T \tag{5}$$

Where,

$$OF_2 = min\left(\sum_{t=1}^{24} ALC(t)\right) \tag{6}$$

The Total Voltage Variation (TVV) can be defined as [30]:

$$TVV(i) = \sum_{i=2}^{N_{bus}} |1 - V_i| \tag{7}$$

Where,

$$OF_3 = min\left(\sum_{t=1}^{24} TVV(t)\right) \tag{8}$$

2.2 Power balance constraint

Equality constraints are represented by the power balance equations [29-32]:

$$P_G + P_{DG} = P_D + P_{Loss} \tag{9}$$

$$Q_G = Q_D + Q_{Loss} \tag{10}$$

2.3 Distribution line constraints

Inequality constraints are represented by the distribution line [5-12]:

$$V_{min} \leq |V_i| \leq V_{max} \tag{11}$$

$$\left|V_1 - V_j\right| \leq \Delta V_{max} \tag{12}$$

$$\left|S_{ij}\right| \leq |S_{max}| \tag{13}$$

2.4 PV-DG constraints

Inequality constraints of PV source-based DG [27-32]:

$$P_{DG}^{min} \leq P_{DG} \leq P_{DG}^{max} \tag{14}$$

$$2 \leq DG_{Position} \leq N_{Bus} \tag{15}$$

$$N_{DG} \leq N_{DG.max} \tag{16}$$

$$n_{DG,i}/Location \leq 1 \tag{17}$$

3. Description of various CSSA

In this section, a novel hybridization approach based on the SSA algorithm and chaos theory based on various chaotic maps.

3.1 Mathematical model of basic SSA

The population of salps *X* consists of *N* agents with *d*-dimensions as described in the following equation [17]:

$$X_i = \begin{bmatrix} x_1^1 & x_2^1 & \cdots & x_d^1 \\ x_1^2 & x_2^2 & \cdots & x_d^2 \\ \vdots & \vdots & \cdots & \vdots \\ x_1^N & x_2^N & \cdots & x_d^N \end{bmatrix} \tag{18}$$

In basic SSA, the position of the leader is updated according to the follows [17, 33]:

$$X_i^1 = \begin{cases} F_i + c_1[(ub_i - lb_i)c_2 + lb_i] & c_3 \geq 0 \\ F_i - c_1[(ub_i - lb_i)c_2 + lb_i] & c_3 < 0 \end{cases} \tag{19}$$

The first coefficient c_1 is introduced to make a balance between the exploration and the exploitation is defined in flowing equation:

$$c_1 = 2.e^{-\left(\frac{4k}{k_{\max}}\right)^2} \tag{20}$$

The follower salps update their positions based on Newton's law of motion using the following equation:

$$X_i^k = \frac{1}{2}\left(X_i^k + X_i^{k-1}\right) \qquad 2 \leq k \leq N \tag{21}$$

3.2 Mathematical model of chaotic SSA

The analysis of chaotic dynamical systems is referred to as chaos theory. Nonlinear dynamical systems that are particularly sensitive to their initial conditions are known as chaotic systems. In other words, minor variations in the initial conditions lead to large variations in the system's outcome. In other words, deterministic systems may exhibit chaotic behavior as well. In other words, deterministic systems may exhibit chaotic behavior as well. These characteristics have recently been used to improve optimization algorithms efficiency [34].

Integrating chaos theory into population-based algorithms is one of the cheapest methods for improving both discovery and exploitation, according to the literature [35-37]. The chaotic SSA algorithm combines the local search ability of the chaos operator (CS) and the global search ability of the SSA algorithm [38]. This is the motivation of this study whereby we employ various chaotic maps to improve the performance of the SSA algorithm. In this study, chaotic maps are employed to adjust a random c_2 parameter of SSA. These chaotic SSA algorithms are shown in Table 1.

Table 1. Chaotic maps for SSA algorithm applied.

No.	Algorithms	Ref.	Mathematic equation
1	Chaotic-Gauss -SSA	[39]	$c_{k+1} = \begin{cases} 1 & x_k = 0 \\ \dfrac{1}{mod(x_k, 1)} & otherwise \end{cases}$
2	Chaotic-Logistic-SSA	[40]	$x_{k+1} = \alpha x_k(1 - x_k)$
3	Chaotic-Tent-SSA	[41]	$c_{k+1} = \begin{cases} \dfrac{x_k}{0.7} & , x_k < 0.7 \\ \dfrac{10}{3}(1 - x_k), & x_k \geq 0.7 \end{cases}$
4	Chaotic-Sine-SSA	[42]	$c_{k+1} = \dfrac{\alpha}{4}\sin(\pi x_i)$
5	Chaotic-Singer-SSA	[43]	$c_{k+1} = \mu\left(\begin{matrix} 7.86x_k - 23.31x_k^2 + \\ 28.75x_k^3 - 13.302875x_k^4 \end{matrix}\right)$

The steps of chaotic SSA can be described by the flowchart shown in Figure 1.

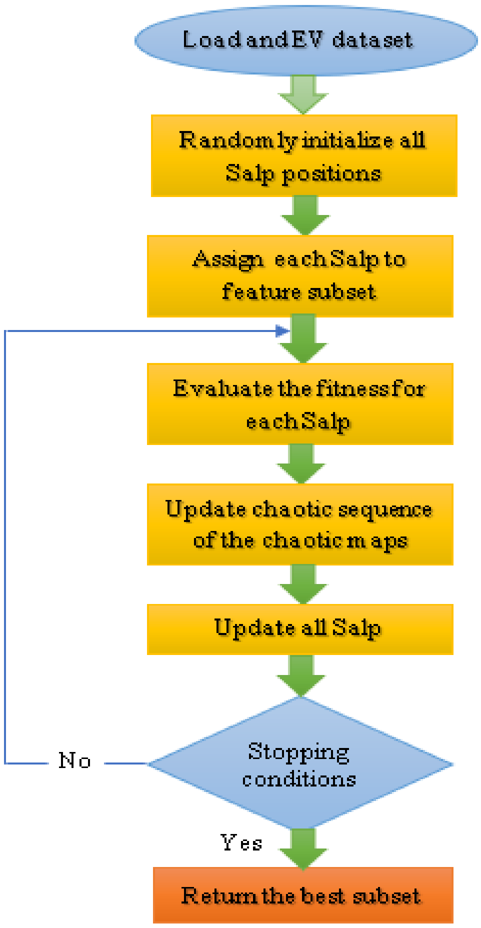

Fig. 1. Flowchart of the proposed chaotic SSA algorithm.

Different time-varying updating strategies for the random values in various chaotic SSA algorithms are traced in Figure 2.

The variance of the random value varies according to the trajectory of each applied chaotic method, as seen in the equations of Table 1, with all methods varying from 0 to 1 in nearly every iteration except for the Gauss method.

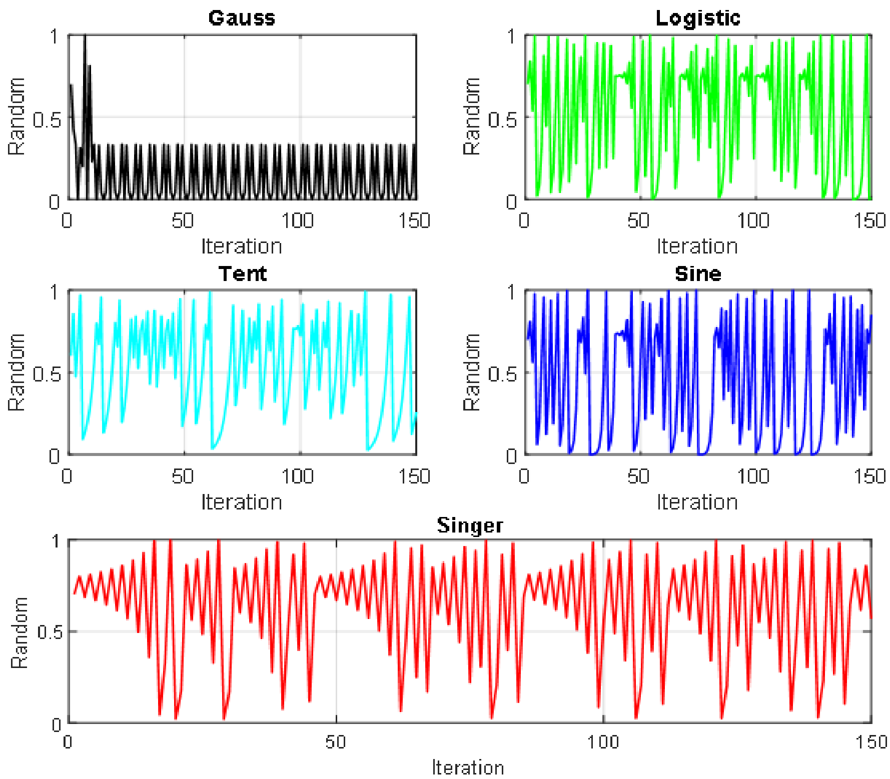

Fig. 2. The random variation for different chaotic SSA applied.

4. Results and discussion

Figure 3 is represented the standard IEEE 69 bus EDS test system. The base MVA and the bus voltage are 10 MVA and 12.66 kV. The proposed chaotic SSA algorithms are implemented in MATLAB.

The five EV charging stations are installed in buses number 18, 26, 31, 43, and 62 with maximum power injected is 327 kW, and with a power factor of 0.82.

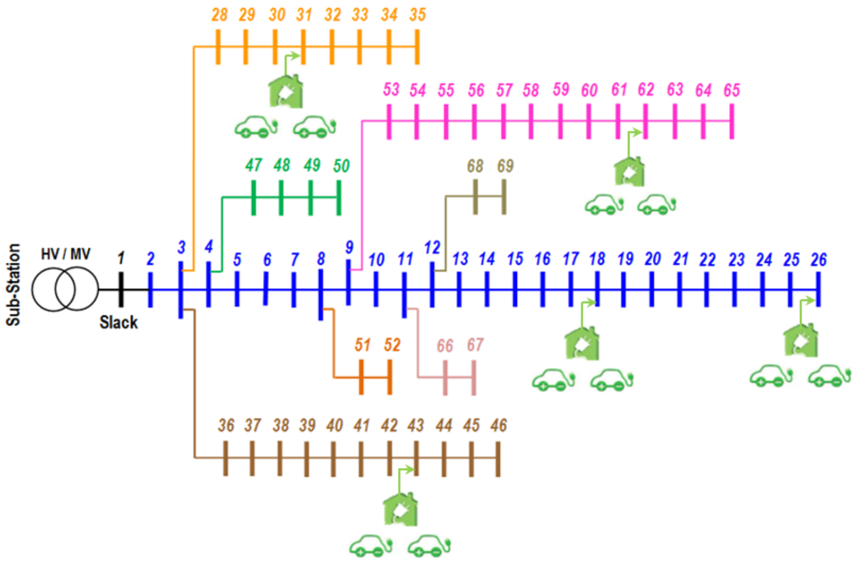

Fig. 3. Single line diagram of the distribution test system with EV charging stations.

For solving this problem, the EDS is assumed to follow a daily load power demand EV charging station curves as shown in Figures 4 and 5, respectively. The power outputs of PV-based DG are assumed to follow the nominalized average output curve shown in Figure 6.

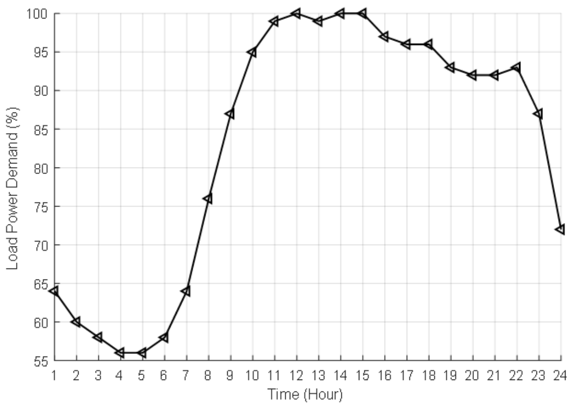

Fig. 4. Daily load demand variation.

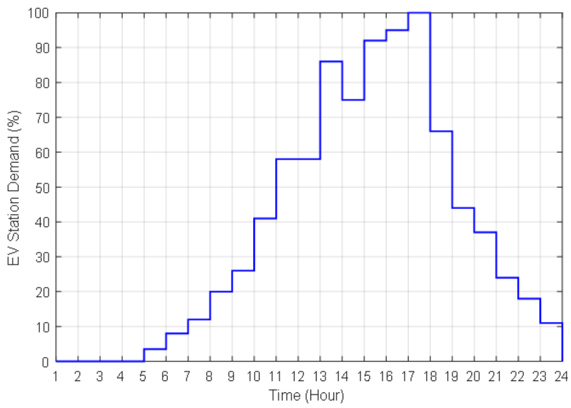

Fig. 5. Daily EV charging station variation.

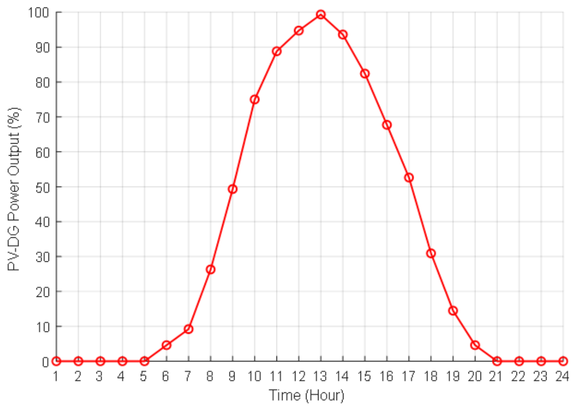

Fig. 6. The daily power output of PV-DG variation.

4.1 Assessment of the competitive algorithms

Figure 7 shows the convergence curve for the MOF minimization, where the best execution results for all chaotic SSA algorithms applied are used.

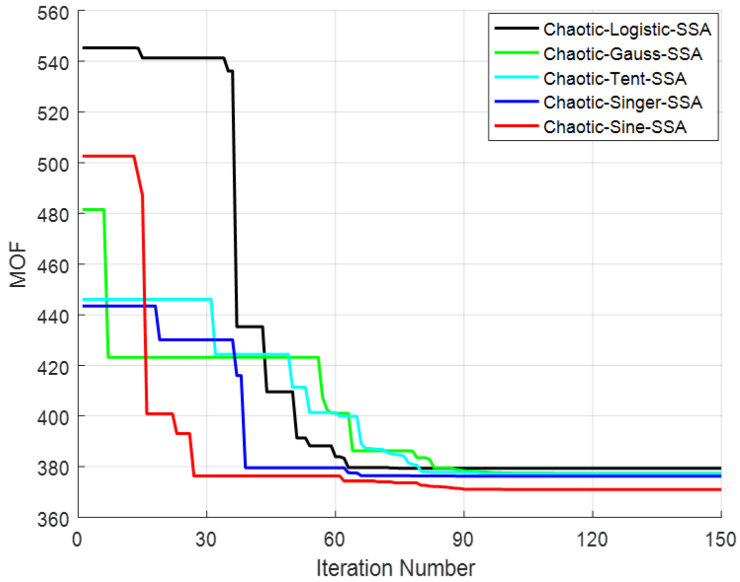

Fig. 7. Convergence curves for various algorithms.

As shown in Figure 7, all algorithms converge quickly within 90 iterations, it is clear that the chaotic logistic-SSA algorithm converges quickly compared to other algorithms, in less than 65 iterations, but it is observed that the chaotic sine-SSA algorithm exhibit the best results of MOF value.

Figure 8 illustrates the boxplot of MOF while using different chaotic SSA algorithms for the EDS test system.

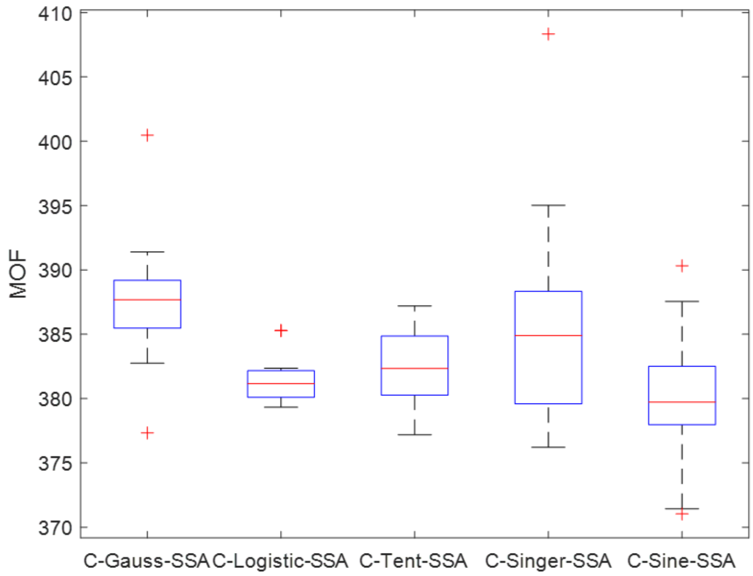

Fig. 8. Boxplot of MOF for various algorithms.

The boxplot shows that all the proposed chaotic algorithms converged to near to their best results of MOF obtained in each of all the 20 executions. Other observations indicate that among the proposed algorithms the minimum value of MOF is obtained for the chaotic sine-SSA.

4.2 Statistical analysis of applied algorithms

Table 2 is represented the mean, best, and worst results of MOF as well as, the rank of the proposed algorithms after integration of DG. The Chaotic-Sine-SSA algorithm has the best result of MOF which proves the efficiency of this algorithm compared to others, this is what made it be in rank 1.

Table 2. Statistical assessment for the competitive algorithms.

Algorithms Applied	Mean	Best	Worst	CPU Time (sec)	Rank
Chaotic-Gauss -SSA	382.7443	379.3266	384.2383	478.32594	5
Chaotic-Logistic-SSA	379.4699	377.3298	380.6880	478.56920	4
Chaotic-Tent-SSA	377.4662	377.1886	380.2597	484.71273	3
Chaotic-Singer-SSA	378.6962	376.2044	379.8982	417.89554	2
Chaotic-Sine-SSA	371.4342	371.0306	376.0256	428.66019	1

4.3 Optimal results

The optimization results of the proposed various chaotic SSA algorithms are represented in Table 3.

Table 3. Optimization results for various algorithms.

Parameters	Chaotic-Gauss -SSA	Chaotic-Logistic-SSA	Chaotic-Tent-SSA	Chaotic-Singer-SSA	Chaotic-Sine-SSA
	1.1263	0.7786	0.7423	0.4136	0.7192
P_{DG} (MW)	1.4337	0.3545	0.3838	0.7778	0.4015
	1.8357	1.8234	1.8388	1.8252	1.8363
DG Buses	18-47-61	17-26-61	18-26-61	14-22-61	18-26-61
$\sum P_{DG}$ (MW)	4.3957	2.9565	2.9649	3.0166	2.9570
$\sum P_{Loss}$ (kW)	3188.2	3175.9	3171.0	3179.3	3172.6
$\sum Q_{Loss}$ (kVar)	1469.4	1467.1	1465.0	1466.9	1465.8
$\sum V_{min}$ (p.u.)	22.6218	22.6185	22.6226	22.6217	22.6216
$\sum$ TVV (p.u.)	35.8971	35.8319	35.8171	35.8208	35.8284
$\sum$ ALC (M.$)	1.6757	1.6693	1.6667	1.6710	1.6675
MOF	379.3266	377.3298	377.1886	376.2044	371.0306

As depicted in Table 3, the best placement obtained by the chaotic sine-SSA algorithm are buses 18, 26, and 61 with a total size of 2.9570 MW, in addition, except for the chaotic gauss-SSA algorithm, the total sizes obtained by the other algorithms are very close, which are vary between 2.9565 MW, and 3.0166 MW, with a difference of 6.01 kW.

Moreover, the best results are obtained by the chaotic-sine-SSA algorithm, which minimizes the sum of P_{Loss} to 3.1726 MW, in addition, the sum, of Q_{Loss}, *TVV*, and *ALC* is minimized to 1465.8 kVar, 35.8284 p.u., 1.6675 M.$ respectively. On the other hand, the chaotic (gauss, logistic, tent, and singer) SSA algorithms recorded the sum of total power losses of 3188.2, 3175.9, 3171.0, and 3179.3 MW. The sum of minimum voltage is obtained for the chaotic-sine-SSA algorithm with 22.6216 p.u.

4.4 Impacts on the electrical distribution system

Figure 9 represents the daily variation of the P_{Loss} in 24 hours for different case studies. From this 3 D graphic, it is clear that the presence of EVCS has a significant influence on the EDS, which leads to an increase in the power losses compared to a basic case especially in buses 7 to 22, and the buses 53 to 64. Where the P_{Loss} is close to 20 kW in bus number 10. On the contrary, the integration of DG leads to reduce the losses of all buses, where the maximum power loss is minimized from 74.0938 kW to 46.2396 kW.

Figure 10 represents the daily voltage profiles of EDS in 24 hours for different case studies. From this figure, the best voltage profiles are obtained in the case of EVCS and DG, which is within the permissible limits especially when in the hours when the DG provide their better active power (noted that these hours are between 8:00 to 18:00).

In addition, the presence of EVCS only leads to minimizing the voltage profiles compared to the basic case that is due to the importance of active and reactive load of EVCS which is 327 kW, and 268.14 kVar, respectively.

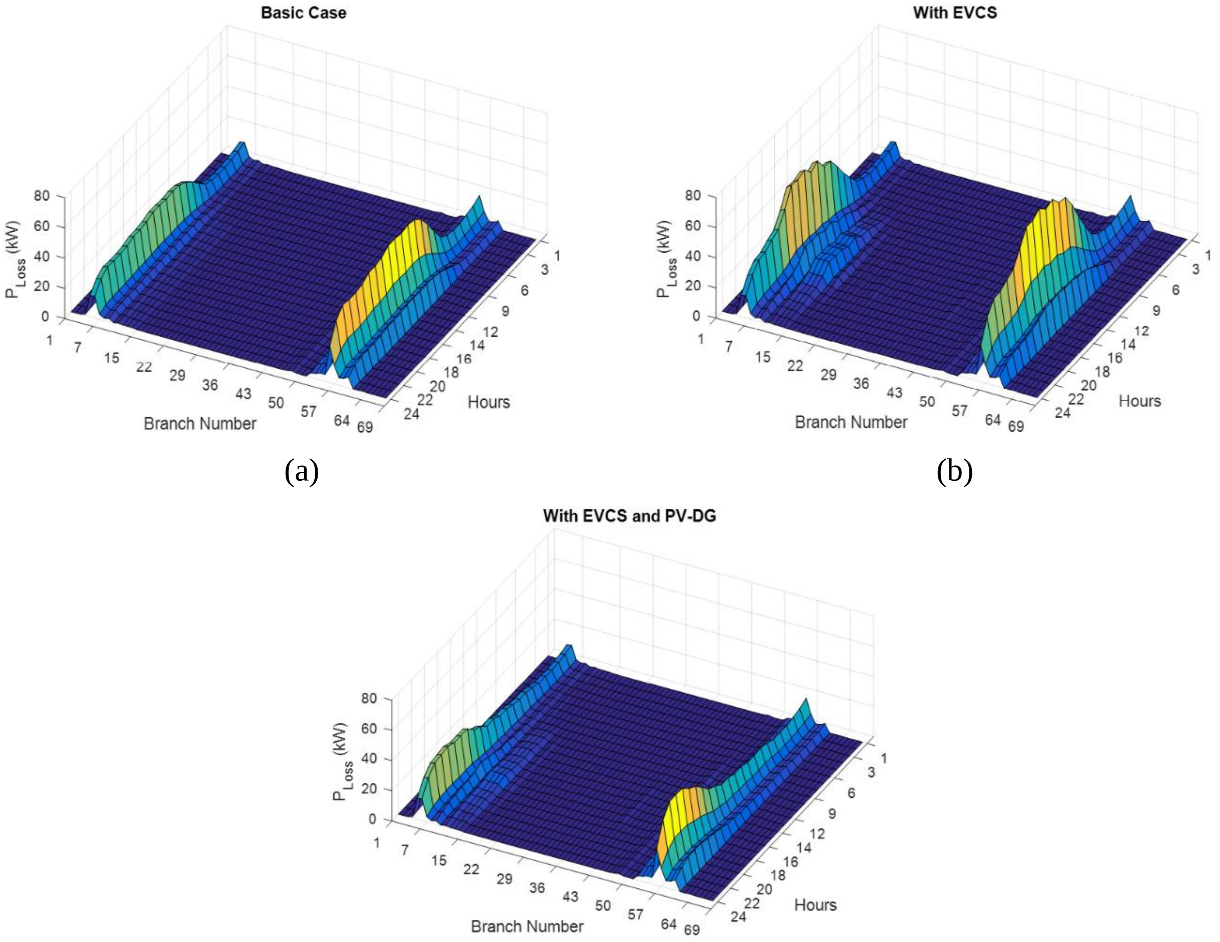

(a) (b)

(c)

Fig. 9. The daily APL for EDS: a). Basic Case, b). With EVCS, c). With EVCS and DGs.

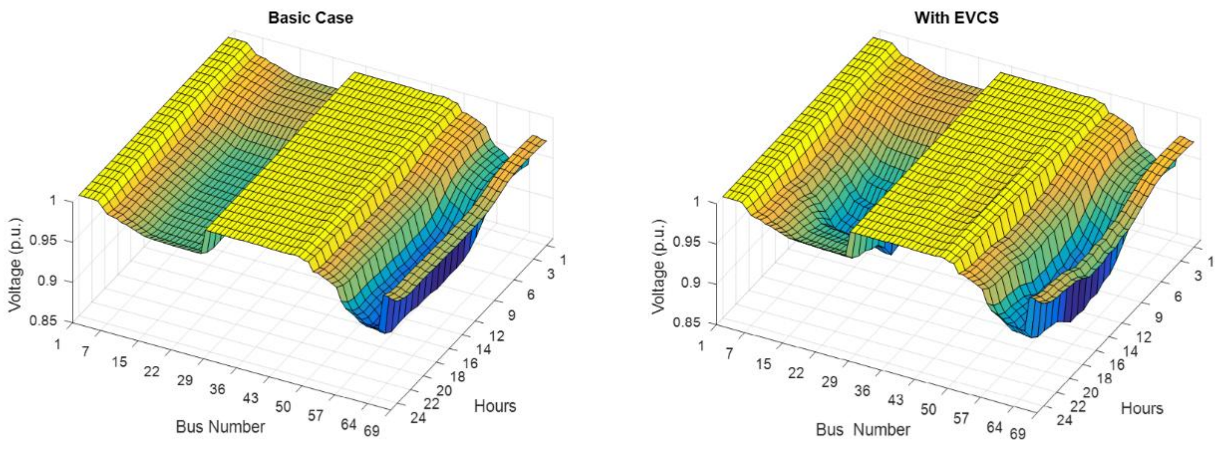

(a) (b)

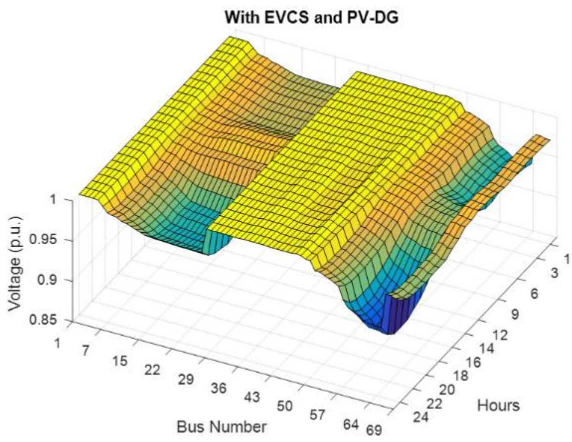

(c)

Fig. 10. Daily bus voltage profiles for EDS: a). Basic Case, b). With EVCS, c). With EVCS and DGs.

Figure 11 illustrates the daily variation of total power losses of EDS for different case studies. From Figure 11.a. the presence of EVCS in EDS increase the P_{Loss} in all the hour of the day which is become close to 430 kW at 15 h after it was 220 kW. But after the integration of multiple DG units, the P_{Loss} value is minimized to less than 155 kW. From Figure 11.b. Also, the existence of EVCS effect on the Q_{Loss}, wherein the basic case the maximum Q_{Loss} was in the range of 100 kVar in the hours from 11:00 to 13:00, while the presence of EVCS increases the amount of Q_{Loss}, which is become more than 140 kVar, whereas the integration of DGs significantly reduces the Q_{Loss}, which is becoming less than 80 kVar. In addition, due to the uncertainty of DG there is no variation in the power losses in the hour between 23:00 to 5:00. On the other hand, the minimum P_{Loss} and Q_{Loss} are obtained at 13 h because in this hour the DG supplied their maximum power injected to EDS.

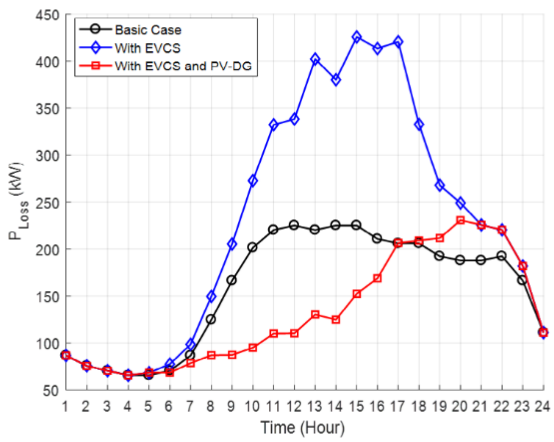

(a)

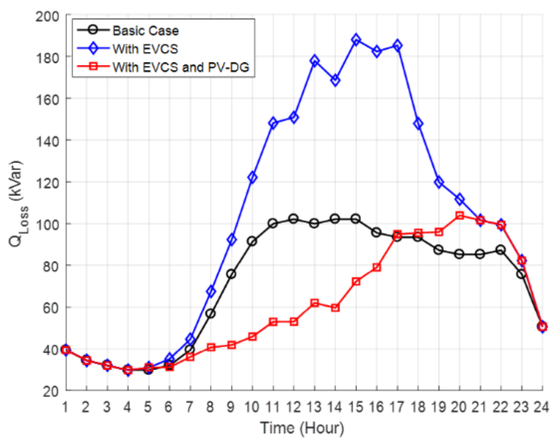

(b)

Fig. 11. The total power losses in 24 h of EDS: a). P_{Loss}, b). Q_{Loss}.

5. Conclusions

This paper addresses the planning optimal location and size of PV based-DG units in EDS with the presence of EVCS by taking into consideration the uncertainties in 24 hours using different chaotic SSA algorithms.

The results obtained show that the allocation and sizing of PV-DG units reduce the power losses and enhance the voltage profile. The simulation results proved the efficiency and robustness of the chaotic sine SSA algorithm compared with other various chaotic SSA algorithms in terms of achieving minimum P_{Loss}, *TVV*, and *ALC* values.

Future work will consider developing the multi-objective CSSA algorithm for more complicated scenarios including the variation of loadability, harmonics source, and the impact of hourly variation of hybrid DG power-based technic, economic and environmental aspects.

Nomenclature

EDS Parameters:

K_P	Incremental cost of power loss (0.06 $/kW)
N_{bus}	Number of buses
P_D, Q_D	Active and reactive power of load
P_G, Q_G	Active and reactive power of generator
P_i, Q_i	Active and reactive power at bus
P_{ij}, Q_{ij}	Active and reactive power in branch
P_{Loss}, Q_{Loss}	Total power losses of EDS
R_{ij}, X_{ij}	Resistance and reactance line
S_{ij}	Apparent power in branch
T	Number of hours per year (8760 h)
V_i, δ_i	Voltage magnitude and angle at bus
V_{min}, V_{max}	Limit of bus voltage
ΔV_{max}	Maximum voltage drops at each branch

PV based DG Parameters:

$DG_{Position}$, N_{DG}	Position and number of DG units
$n_{DG,\,i}$	Location of DG units at bus *i*
P_{DG}	Active power injection from DG
P_{DG}^{min}, P_{DG}^{max}	Limit size of DG

Chaotic SSA Parameters:

c_1	Random of the first balance coefficient
c_2	Random number adjusted by chaotic maps
c_3	Random number
F_i	Place of food source
k, k_{max}	Current and maximum iterations
N	Number of salp particles

ub_i, lb_i	Upper and lower bounds
X_i^1	Leader's position
X_i^k	Position of salp

6. References

[1] Das HS, Rahman MM, Li S, Tan CW. Electric vehicles standards, charging infrastructure, and impact on grid integration: A technological review. Renewable and Sustainable Energy Reviews, 2020; 120: 109618. doi:10.1016/j.rser.2019.109618.

[2] Shepero M, Munkhammara J, Widéna J, Bishopbc JDK, Boströmd T. Modeling of photovoltaic power generation and electric vehicles charging on city-scale: A review. Renewable and Sustainable Energy Reviews, 2018; 89: 61-71. doi:10.1016/j.rser.2018.02.034.

[3] El-Bayeh CZ, Alzaareer K, Brahmi B, Zellagui M. A novel algorithm for controlling active and reactive power flows of electric vehicles in buildings and its impact on the distribution network. World Electric Vehicle Journal, 2020; 11(2): 43. doi: 10.3390/wevj11020043.

[4] Awad AS, Shaaban MF, EL-Fouly THM, El-Saadany EF. Salama MMA. Optimal resource allocation and charging prices for benefit maximization in smart PEV-Parking lots. IEEE Transactions on Sustainable Energy, 2017; 8(3): 906–915. doi: 10.1109/TSTE.2016.2617679.

[5] Luo L, Gu W, Wu Z, Zhou S. Joint planning of distributed generation and electric vehicle charging stations considering real-time charging navigation. Applied Energy, 2019; 242: 1274–1284. doi: 10.1016/j.apenergy.2019.03.162.

[6] Erdinç O. Taşcıkaraoğlu A, Paterakis NG, Dursun I, Sinim MC, Catalao JP. Comprehensive optimization model for sizing and siting of DG units, EV charging stations, and energy storage systems. IEEE Trans. on Smart Grid, 2018; 9(4): 3871–3882. doi: 10.1109/TSG.2017.2777738.

[7] Ahmadian A, Sedghi M, Elkamel A, Aliakbar-Golkar M, Fowler M. Optimal WDG planning in active distribution networks based on Possibility–probabilistic PEVs load modelling. IET Generation, Transmission & Distribution, 2017; 11(4): 865–875. doi: 10.1049/iet-gtd.2016.0778.

[8] Domínguez-Navarro JA, Dufo-López R, Yusta-Loyo JM, Artal-Sevil JS, Bernal-Agustín JL. Design of an electric vehicle fast-charging station with integration of renewable energy

and storage systems. International Journal of Electrical Power & Energy Systems, 2019; 105: 46–58. doi: 10.1016/j.ijepes.2018.08.001.

[9] Liu L, Zhang Y, Da C, Huang Z, Wang M. Optimal allocation of distributed generation and electric vehicle charging stations based on intelligent algorithm and bi- level programming. International Transactions on Electrical Energy Systems, 2020; 30(6): e12366. doi: 10.1002/2050-7038.12366.

[10] Garcia-Guarin J, Infante W, Ma J, Alvarez D, Rivera S. Optimal scheduling of smart microgrids considering electric vehicle battery swapping stations. International Journal of Electrical and Computer Engineering, 2020; 10(5): 5093–5107. doi: 10.11591/ijece.v10i5.pp5093-5107.

[11] Sultana U, Khairuddin AB, Sultana B, Rasheed N, Qazi SH, Malik NR. Placement and sizing of multiple distributed generation and battery swapping stations using grasshopper optimizer algorithm. Energy, 2018; 165: 408–421. doi: 10.1016/j.energy.2018.09.083.

[12] Boonraksa T, Mmary ER, Marungsri B. Optimal design of charging station for electric vehicles integrated with renewable DG. 2nd IEEE International Conference on Electrical Engineering and Automation (ICEEA), 25-26 March 2018, Chengdu, China. doi: 10.2991/iceea-18.2018.19.

[13] Mohamed AAS, El-Sayed A, Metwally H, Selem SI. Grid integration of a PV system supporting an EV charging station using salp swarm optimization. Solar Energy, 2020; 205: 170–182. doi: 10.1016/j.solener.2020.05.013.

[14] Wang S, Yu L, Wu L, Dong Y, Wang H. An improved differential evolution algorithm for optimal location of battery swapping stations considering multi-type electric vehicle scale evolution. IEEE Access, 2019; 7: 73020–73035. doi: 10.1109/ACCESS.2019.2919507.

[15] Hafez O, Bhattacharya K. Optimal design of electric vehicle charging stations considering various energy resources. Renewable Energy, 2017; 107: 576–589. doi: 10.1016/j.renene.2017.01.066.

[16] Battapothula G, Yammani C, Maheswarapu S. Multi-objective optimal planning of FCSs and DGs in distribution system with future EV load enhancement. IET Electrical Systems in Transportation; 2018; 9(3): 128–139. doi: 10.1049/iet-est.2018.5066.

[17] Mirjalili S, Faris H, Gandomi AH, Mirjalili SM, Mirjalili SZ, Saremi S. Salp swarm algorithm: a bio-inspired optimizer for engineering design problems. Advances in Engineering Software, 2017; 114: 163–191. doi: 10.1016/j.advengsoft.2017.07.002.

[18] Elazab OS, Debouza M, Hasanien HM, Muyeen SM, Al-Durra A. Salp swarm algorithm-based optimal control scheme for LVRT capability improvement of grid-connected

photovoltaic power plants: design and experimental validation. IET Renewable Power Generation, 2020; 14(4): 591–599. doi: 10.1049/iet-rpg.2019.0726.

[19] Nayak JR, Shaw B, Sahu BK. Implementation of hybrid SSA-SA based three-degree-of-freedom fractional-order PID controller for AGC of a two-area power system integrated with small hydro plants. IET Generation, Transmission & Distribution, 2020; 14(13): 2430–2440. doi: 10.1049/iet-gtd.2019.0113.

[20] Hasanien HM, El-Fergany AA. Salp swarm algorithm-based optimal load frequency control of hybrid renewable power systems with communication delay and excitation cross-coupling effect. Electric Power Systems Research, 2019; 176: 105938. doi: 10.1016/j.epsr.2019.105938.

[21] Allam D, Mohamed H, Al-Gabalawy M, Eteiba MB. Optimization of voltage source inverter's controllers using salp swarm algorithm in grid connected photovoltaic system. 21st IEEE International Middle East Power Systems Conference (MEPCON), 17-19 December 2019, Cairo, Egypt. doi: 10.1109/MEPCON47431.2019.9008199.

[22] Elattar EE, El Sayed SK. Probabilistic energy management with emission of renewable micro-grids including storage devices based on efficient salp swarm algorithm. Renewable Energy, 2020; 153: 23–35. doi: 10.1016/j.renene.2020.01.144.

[23] Abbassi R, Abbassi A, Heidari A, Mirjalili S. An efficient salp swarm-inspired algorithm for parameters identification of photovoltaic cell models. Energy Conversion and Management, 2019; 179(1): 362–372. doi: 10.1016/j.enconman.2018.10.069.

[24] Kamel S, Nasrat L, Yu J, Xie K, Khasanov M. Radial distribution system reconfiguration for real power losses reduction by using salp swarm optimization algorithm. IEEE Innovative Smart Grid Technologies - Asia (ISGT Asia), 21-24 May 2019, Chengdu, China. doi: 10.1109/ISGT-Asia.2019.8881446.

[25] Gholami K, Parvaneh MH. A mutated salp swarm algorithm for optimum allocation of active and reactive power sources in radial distribution systems. Applied Soft Computing Journal, 2019; 85: 105833. doi: 10.1016/j.asoc.2019.105833.

[26] Khaboot N, Srithapon C, Siritaratiwat A, Khunkitti P. Increasing benefits in high PV penetration distribution system by using battery energy storage and capacitor placement based on salp swarm algorithm. Energies, 2019; 12(24): 1–20. doi: 10.3390/en12244817.

[27] Qais MH, Hasanien HM, Alghuwainem S. Enhanced salp swarm algorithm: Application to variable speed wind generators. Engineering Applications of Artificial Intelligence, 2019; 80: 82–96. doi: 10.1016/j.engappai.2019.01.011.

[28] Yang B, Zhong L, Zhang X, Shu H, Yu T, Li H, Jiang L, Sun L. Novel bio-inspired memetic salp swarm algorithm and application to MPPT for PV systems considering partial shading condition. Journal of Cleaner Production, 2019; 215: 1203–1222. doi: 10.1016/j.jclepro.2019.01.150.

[29] Lasmari A, Zellagui M, Hassan HA, Settoul S, Abdelaziz AY, Chenni R. Optimal energy-efficient integration of photovoltaic DG in radial distribution systems for various load models. 11th International Renewable Energy Congress (IREC), 29-31 October 2020, Hammamet, Tunisia. doi: 10.1109/IREC48820.2020.9310429.

[30] Lasmari A, Settoul S, Zellagui M, Chenni R. Optimal hourly scheduling of PV sources in EDS considering the power variability of load demand and DG using MOGWO algorithm. 6th International Conference on Electric Power and Energy Systems (EPECS), 5-7 October 2020, Istanbul, Turkey. doi: 10.1109/EPECS48981.2020.9304970.

[31] Settoul S, Chenni R, Hassan HA, Zellagui M, Kraimia MN. MFO algorithm for optimal location and sizing of multiple photovoltaic distributed generations units for loss reduction in distribution systems. 7th International Renewable and Sustainable Energy Conference (IRSEC), 30-27 November, Agadir, Morocco. doi: 10.1109/IRSEC48032.2019.9078241.

[32] Lasmari A, Zellagui M, Chenni R, Semaoui S, El-Bayeh CZ, Hassan HA. Optimal energy management system for distribution systems using simultaneous integration of PV-based DG and DSTATCOM units. Energetika, 2020; 66(1): 1–14. doi: 10.6001/energetika.v66i1.4294.

[33] Faris H, Mirjalili S, Aljarah I, Mafarja M, Heidari AA. Salp swarm algorithm: theory, literature review, and application. In: extreme learning machines. Studies in Computational Intelligence; 2020, p. 185–199. doi: 10.1007/978-3-030-12127-3_11.

[34] Mirjalili S, Gandomi AH. Chaotic gravitational constants for the gravitational search algorithm. Applied Soft Computing, 2017; 53: 407–419. doi: 10.1016/j.asoc.2017.01.008.

[35] Alatas B. Chaotic bee colony algorithms for global numerical optimization. Expert Systems with Applications, 2010; 37(8): 5682–5687. doi: 10.1016/j.eswa.2010.02.042.

[36] Zellagui M, Lasmari A, Settoul S, El-Bayeh CZ, Chenni R. Assessment integration of hybrid PV-DSTATCOM-BES-DG system in EDS under uncertainties using chaotic adaptive inertia weight PSO algorithms. 12th International Symposium on Advanced Topics in Electrical Engineering (ATEE), 25-27 March 2021, Romania, doi: 10.1109/ATEE52255.2021.9425344.

[37] Settoul S, Zellagui M, Chenni R. A new optimization algorithm for optimal wind turbine location problem in Constantine city electric distribution network based active power loss

reduction. Journal of Optimization in Industrial Engineering, 2021; 14 (2): 13–22. doi:10.22094/joie.2020.1892184.1725.

[38] Sayed GI, Khoriba G, Haggag MH. A novel chaotic salp swarm algorithm for global optimization and feature selection. Applied Intelligence, 2018; 48: 3462–3481. doi: 10.1007/s10489-018-1158-6.

[39] Koyuncu H. GM-CPSO: A new viewpoint to chaotic particle swarm optimization via gauss map. Neural Processing Letters, 2020; 52: 241–266. doi: 10.1007/s11063-020-10247-2.

[40] Zhenyu G, Bo C, Min Y, Binggang C. Self-adaptive chaos differential evolution. Lecture Notes in Computer Science, 2006; 4221: 972–975. doi: 10.1007/11881070_128.

[41] Teh JS, Samsudin A, Akhavan A. Parallel chaotic hash function based on the shuffle-exchange network. Nonlinear Dynamics, 2015; 81(3): 1067–1079. doi: 10.1007/s11071-015-2049-6.

[42] Chen K, Zhou F, Liu A. Chaotic dynamic weight particle swarm optimization for numerical function optimization. Knowledge-Based Systems, 2018; 139: 23–40. doi: 10.1016/j.knosys.2017.10.011.

[43] Ibrahim RA, Oliva D, Ewees AA, Lu S. Feature selection based on improved runner-root algorithm using chaotic singer map and opposition-based learning. Lecture Notes in Computer Science, 2017; 10638: 156–166. doi: 10.1007/978-3-319-70139-4_16.